

## Efficient quantum repeater based on deterministic Rydberg gates

Bo Zhao,<sup>1,2</sup> Markus Müller,<sup>1,2</sup> Klemens Hammerer,<sup>1,2</sup> and Peter Zoller<sup>1,2</sup>

<sup>1</sup>*Institute for Theoretical Physics, University of Innsbruck, A-6020 Innsbruck, Austria*

<sup>2</sup>*Institute for Quantum Optics and Quantum Information of the Austrian Academy of Sciences, A-6020 Innsbruck, Austria*

(Received 9 March 2010; published 21 May 2010)

We propose an efficient quantum repeater architecture with mesoscopic atomic ensembles, where the Rydberg blockade is employed for deterministic local entanglement generation, entanglement swapping, and entanglement purification. Compared to a conventional atomic-ensemble-based quantum repeater, the entanglement distribution rate is improved by up to two orders of magnitude with the help of the deterministic Rydberg gate. This quantum repeater scheme is robust and fast, and thus opens up a way for practical long-distance quantum communication.

DOI: [10.1103/PhysRevA.81.052329](https://doi.org/10.1103/PhysRevA.81.052329)

PACS number(s): 03.67.Hk, 03.67.Pp, 42.50.Ex

### I. INTRODUCTION

Quantum information can be transmitted *directly* over distances above some hundred kilometers only at unpractically low rates due to loss and decoherence. In order to remedy this limitation, the concept of a quantum repeater has been introduced [1], where quantum entanglement is distributed over small distances, stored in quantum memories, purified, and swapped in a nested architecture [2]. A quantum repeater can in principle be implemented only with atomic ensembles and linear optics [3]. However, despite significant progress during the last years on both the theoretical [4–6] and experimental side [7,8] (see [9,10] for recent reviews), the entanglement distribution rate achievable in such an architecture is still much too inefficient to be of practical interest, even under ideal conditions. This is predominantly due to the fact that linear optical methods only allow for a probabilistic entanglement manipulation, posing severe limitations on the overall success probability and, therefore, on the rate of entanglement distribution.

In this paper, we introduce a deterministic quantum repeater protocol using quantum gates for entanglement swapping and purification. The quantum gates rely on the Rydberg blockade effect in mesoscopic atomic ensembles [11] and the remarkable recent advances in exploiting this effect for quantum information processing [12–16]. Deterministic operation provides an enhancement of two orders of magnitude in the rate of entanglement distribution compared with the best quantum repeater based on linear optics [5]. For realistic local errors around  $10^{-3}$ – $10^{-2}$ , this quantum repeater architecture yields a rate of about 10 ebits per s. We thus show that deterministic quantum repeaters based on Rydberg gates open up an avenue for high-rate, long-distance quantum communication.

Deterministic quantum gates based on trapped ions were recently explored in [17] in the context of quantum repeaters. However, this requires strong coupling between single ions and high-finesse cavities, which is still challenging for current technology. The use of Rydberg gates in quantum repeaters was first proposed in [18]. In this protocol, the distribution of entanglement at the fundamental repeater level is still probabilistic as it is based on the absorption of photons which are lost in the channel in most cases. The gate operation therefore has to rely on postselection, just as the conventional protocols based on linear optics [9]. In contrast, the quantum repeater architecture introduced here is deterministic, does not

require strong coupling between atoms and light, and is robust against path length fluctuations.

In our protocol, mesoscopic atomic ensembles of the size of a few micrometers are exploited as a quantum memory. If the atoms in such ensembles are laser excited to high-lying Rydberg states, strong and long-range van der Waals or dipole-dipole interactions give rise to the Rydberg blockade, which prevents the excitation of more than one Rydberg atom within a volume, which is smaller than the blockade radius [11,16]. Based on the large nonlinearity associated with the blockade effect, deterministic entangling quantum gates can be performed between collective excited states in one or different atomic ensembles by applying a series of collective and single-atom laser pulses [12]. Our protocol starts with local and deterministic entanglement generation in one atomic ensemble with the help of a collective Rydberg gate. The entanglement is then linked between neighboring sites by linear optical methods, where two-photon interference is explored. Further entanglement swapping and entanglement purification are implemented based on Rydberg gates between two nearest-memory atomic ensembles at one site. The protocol presented here is improved in three respects compared with conventional schemes: (i) local entanglement manipulation is performed deterministically, (ii) the number of times required to convert atomic states into photons is reduced to a minimum, and (iii) the detection step in entanglement swapping and entanglement purification can be performed with the help of field ionization, thereby significantly increasing the detection efficiency.

### II. BASIC PROTOCOL

We envision a setup with mesoscopic cold atomic ensembles with a diameter of several microns. The relevant energy levels are shown in Fig. 1(a) and comprise an electronic ground-state manifold with five sublevels,  $|g\rangle$ ,  $|s\rangle$ ,  $|s'\rangle$ ,  $|t\rangle$ , and  $|t'\rangle$ , and two Rydberg states which we denote by  $|r\rangle$  and  $|r'\rangle$ . Initially all the atoms are prepared in the ground state,  $|g\rangle$ . We assume these sublevels can be addressed individually and that atoms in the two Rydberg states experience strong interactions.

In our scheme, we first generate a qubit-type entanglement in one atomic ensemble, which can be done as follows [see Fig. 1(a)]:

i. A collective  $\pi$  pulse (Rabi frequency  $\Omega_N \propto \sqrt{N}$ ) and a single-atom  $\pi$  pulse are applied sequentially to create one

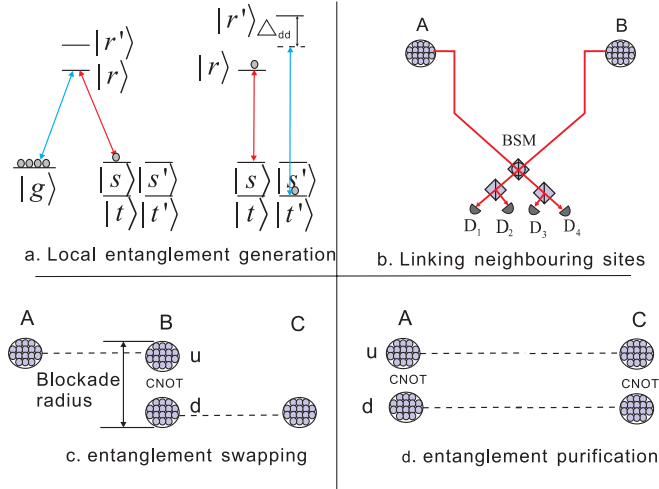


FIG. 1. (Color online) Schematic view of the quantum repeater protocol with mesoscopic atomic ensembles based on a Rydberg gate, including local entanglement generation, entanglement linking, entanglement swapping, and entanglement purification.

collective excitation, transferring  $|\mathbf{0}\rangle \rightarrow |\mathbf{r}\rangle \rightarrow |\mathbf{s}\rangle$ , where  $|\mathbf{0}\rangle = |g, \dots, g\rangle$ , and  $|\mathbf{x}\rangle = \frac{1}{\sqrt{N}} \sum_{i=1}^N |g, \dots, g, x_i, g, \dots, g\rangle$ , where  $x = r, r', s, t, s',$  or  $t'$  represents the collective state. In the intermediate step, the Rydberg blockade prevents excitation of more than one atom.

ii. We create a second collective excitation  $|\mathbf{t}'\rangle$  with the same method.

iii. A single-atom  $\pi/2$  pulse transfers  $|\mathbf{s}\rangle$  to  $(|\mathbf{s}\rangle + |\mathbf{r}\rangle)/\sqrt{2}$ .

iv. A single-atom  $\pi$  pulse excites  $|\mathbf{t}'\rangle$  to  $|\mathbf{r}'\rangle$ . Due to dipole blockade, we obtain  $(|\mathbf{s}\rangle|\mathbf{r}'\rangle + |\mathbf{r}\rangle|\mathbf{t}'\rangle)/\sqrt{2}$ .

v. Finally, we apply two single-atom  $\pi$  pulses to bring  $|\mathbf{r}'\rangle$  to  $|\mathbf{s}'\rangle$ , and  $|\mathbf{r}\rangle$  to  $|\mathbf{t}\rangle$ , and obtain the desired Bell state  $(|\mathbf{s}\rangle|\mathbf{s}'\rangle + |\mathbf{t}\rangle|\mathbf{t}'\rangle)/\sqrt{2}$ .

In a second step, all pairs of nearest communication sites are linked using methods from linear optics [4,5]: After the generation of local entanglement at sites, say, A and B, light pulses are read and applied to convert the collective excitations in  $|\mathbf{s}'\rangle$  and  $|\mathbf{t}'\rangle$  into photons with different polarization (e.g.,  $|H\rangle$  and  $|V\rangle$ , respectively) such that the whole system is described by  $(|\mathbf{s}_A\rangle|H_A\rangle + |\mathbf{t}_A\rangle|V_A\rangle)(|\mathbf{s}_B\rangle|H_B\rangle + |\mathbf{t}_B\rangle|V_B\rangle)/2$ . The two photons from both sites are directed to the middle point and detected in a Bell state analyzer composed of a polarizing beam splitter and single-photon detectors [4], where two of the Bell states, for example,  $(|H_A\rangle|H_B\rangle \pm |V_A\rangle|V_B\rangle)/\sqrt{2}$ , are identified [see Fig. 1(b)]. Once a two-photon coincidence count between the single-photon detectors (e.g.,  $D_1$  and  $D_4$ ) is registered, entanglement is generated between two memory qubits at neighboring sites, described by  $|\phi\rangle_{A,B} = (|\mathbf{s}_A\rangle|\mathbf{s}_B\rangle + |\mathbf{t}_A\rangle|\mathbf{t}_B\rangle)/\sqrt{2}$ . This process is heralded, with a success probability of  $p = \frac{1}{2}\eta_r^2\eta_{pd}^2\eta_{att}^2$ , where  $\eta_r$  is the retrieval efficiency,  $\eta_{pd}$  is the photon detection efficiency, and  $\eta_{att} = e^{-L_0/(2L_{att})}$  denotes the loss in the photonic channel where  $L_{att}$  is the attenuation length. If no coincidence is registered, the local entanglement generation and linking steps are repeated until success is achieved.

Finally, after neighboring communication sites are linked, we can connect them by entanglement swapping. Suppose we have generated entanglement  $|\phi\rangle_{AB_u}$  and  $|\phi\rangle_{B_dC}$  between

TABLE I. Truth table of the CNOT gate operation between two ensembles located at the same communication site, required for entanglement swapping. The steps involving the Rydberg blockade mechanism are denoted by  $\Rightarrow$ .

$\mathbf{s}_{B_u}\mathbf{s}_{B_d}$	$\rightarrow \mathbf{r}_{B_u}\mathbf{s}_{B_d}$	$\Rightarrow \mathbf{r}_{B_u}\mathbf{s}_{B_d}$	$\rightarrow \mathbf{r}_{B_u}\mathbf{s}_{B_d}$	$\Rightarrow \mathbf{r}_{B_u}\mathbf{s}_{B_d}$	$\rightarrow \mathbf{s}_{B_u}\mathbf{s}_{B_d}$
$\mathbf{s}_{B_u}\mathbf{t}_{B_d}$	$\rightarrow \mathbf{r}_{B_u}\mathbf{t}_{B_d}$	$\Rightarrow \mathbf{r}_{B_u}\mathbf{t}_{B_d}$	$\rightarrow \mathbf{r}_{B_u}\mathbf{t}_{B_d}$	$\Rightarrow \mathbf{r}_{B_u}\mathbf{t}_{B_d}$	$\rightarrow \mathbf{s}_{B_u}\mathbf{t}_{B_d}$
$\mathbf{t}_{B_u}\mathbf{s}_{B_d}$	$\rightarrow \mathbf{t}_{B_u}\mathbf{s}_{B_d}$				
$\mathbf{t}_{B_u}\mathbf{t}_{B_d}$	$\rightarrow \mathbf{t}_{B_u}\mathbf{t}_{B_d}$				

atomic ensembles A and  $B_u$ , and  $B_d$  and C, as shown in Fig. 1(c). The two atomic ensembles at site B are placed close to each other within the blockade radius, so that we can perform a two-qubit gate between them. To implement entanglement swapping, we first apply a controlled-NOT (CNOT) gate between the memory qubits stored in atomic ensembles  $B_u$  and  $B_d$ , which can be done by a series of single-atom  $\pi$  pulses [19]: (i) a  $\pi$  pulse excites  $|\mathbf{s}_{B_u}\rangle$  to  $|\mathbf{r}_{B_u}\rangle$ , (ii) a  $\pi$  pulse brings  $|\mathbf{s}_{B_d}\rangle$  to  $|\mathbf{r}_{B_d}\rangle$ , (iii) a  $\pi$  pulse transfers  $|\mathbf{r}_{B_d}\rangle$  and  $|\mathbf{t}_{B_d}\rangle$ , (iv) a  $\pi$  pulse transfers  $|\mathbf{r}_{B_d}\rangle$  to  $|\mathbf{s}_{B_d}\rangle$ , and (v) a final  $\pi$  pulse returns  $|\mathbf{r}_{B_u}\rangle$  to  $|\mathbf{s}_{B_u}\rangle$ . The corresponding truth table is shown in Table I.

After applying the CNOT gate, we measure the memory qubits in the ensembles  $B_u$  and  $B_d$  in four states,  $|+_{B_u}\rangle|\mathbf{s}_{B_d}\rangle$ ,  $|-_{B_u}\rangle|\mathbf{s}_{B_d}\rangle$ ,  $|+_{B_u}\rangle|\mathbf{t}_{B_d}\rangle$ , and  $|-_{B_u}\rangle|\mathbf{t}_{B_d}\rangle$ , where  $|\pm_{B_u}\rangle = (|\mathbf{s}_{B_u}\rangle \pm |\mathbf{t}_{B_u}\rangle)/\sqrt{2}$ , in order to project the memory qubits at sites A and C into the desired entangled state. In contrast to conventional schemes where the collective excitations are converted into photons for the detection, we suggest measuring the quantum state by transferring the excitation to a Rydberg state, field-ionizing the atom, and detecting the ions. Detection of single Rydberg atoms has been demonstrated in a photon counting experiment with near-unity detection efficiencies  $\eta_d$  [20]. After the detection, the states are projected into  $(|\mathbf{s}_A\rangle|\mathbf{s}_C\rangle + |\mathbf{t}_A\rangle|\mathbf{t}_C\rangle)/\sqrt{2}$ , up to a local unitary transformation.

The communication distance can be extended further by entanglement swapping. Since entanglement swapping is deterministic, the entanglement distribution rate is similar to that of a quantum repeater based on trapped ions [17]. For  $L = 2^n L_0$ , the total time needed can be approximated by

$$T_{\text{tot}} \approx \prod_{i=0}^n \alpha_i \frac{T_{\text{cc}}}{p} \approx \frac{\prod_{i=1}^n \alpha_i}{2^{n-1}c} \frac{3L}{\eta_r^2\eta_{pd}^2 e^{-L/(2^n L_{att})}}, \quad (1)$$

where  $T_{\text{cc}} = \frac{L_0}{c}$  is the classical communication time with  $c$  the light speed,  $p = \frac{1}{2}\eta_r^2\eta_{pd}^2\eta_{att}^2$ , and  $\alpha_0/p$  are the average of times that must be repeated before entanglement is successfully linked over the entire distance, with a numerical result of  $\alpha_0 \approx 3$  for  $p \ll 1$ .<sup>1</sup> The coefficients  $\alpha_{i \neq 0} > 1$  denote the average number of attempts needed to implement entanglement swapping due to nonunity detection efficiency.

<sup>1</sup>We first randomly generate  $m$  numbers according to a Bernoulli distribution with a success probability of  $p$ . We then generate  $m'$  numbers according to a Bernoulli distribution, where  $m' = m - k$  with  $k$  the number of “1” events in the last step. This procedure is repeated until finally  $m' = 0$ . The average number of times needed gives  $\alpha_0/p$ . The coefficients  $\alpha_{i \neq 0}$  are determined similarly.

### III. ERROR ANALYSIS AND PURIFICATION

Let us now take into account local manipulation errors, which have been neglected in the discussion so far. The intrinsic errors in local manipulation are mainly induced by decay of the atoms when they are excited to Rydberg states, the imperfect Rydberg blockade induced by finite dipole-dipole shifts [19], and the imprecision of the collective pulses caused by an uncertainty of the atom number  $N$ . The decay of the Rydberg states causes decoherence errors proportional to the Rydberg states' decay rate  $\gamma$  and inversely proportional to the Rabi frequency of the collective pulses  $\Omega_N$  or single-atom pulses  $\Omega_s$ . The finite value of the Rydberg interaction energy shift  $\Delta_{dd}$  (imperfect blockade) will cause several kinds of errors. The first error is that two excitations may be generated in the atomic ensembles and thus cause losses. Second, the adiabatic elimination of the doubly excited Rydberg states will cause an ac Stark shift on the single-atom excitation states, thus causing dephasing errors. These errors in the local entanglement generation step are of the order  $\Omega_{N,s}^2/\Delta_{dd}^2$  and can be estimated as

$$E_{\text{loc}} = 1 - F_{\text{loc}} = 2\frac{\gamma\pi}{\Omega_N} + \frac{\gamma\pi}{\Omega_s} + 4\frac{\Omega_N^2}{\Delta_{dd}^2} + 2\frac{\Omega_s^2}{\Delta_{dd}^2}, \quad (2)$$

with  $F_{\text{loc}}$  the fidelity of the locally achieved entanglement. The imprecision of the collective  $\pi$  pulses is on the order of  $1/N$  for an uncertainty of the atom numbers  $\sqrt{N}$ . For  $N > 100$ , this error is less than 1% and can be safely neglected. In Fig. 2(a), we plot the optimized local errors  $E_{\text{loc}}$  versus  $\Delta_{dd}$  for  $\tau = 1/(2\pi\gamma) = 200$  and  $300 \mu\text{s}$  (and  $\Omega_N = \Omega_s$ ). One can see that the local error is only a few percent for a dipole shift of  $\Delta_{dd} = 20$ – $100$  MHz.

Local imperfections are mainly decoherence, dephasing, and loss errors. We can thus neglect spin-flip errors and describe the local entanglement by a mixed entangled state

$$\rho = [1 - (p_1 + p_0)]\rho_2 + p_1\rho_1 + p_0\rho_0, \quad (3)$$

where  $\rho_2 = F_{\text{loc}}|\phi^+\rangle\langle\phi^+| + (1 - F_{\text{loc}})|\phi^-\rangle\langle\phi^-|$  with  $|\phi^\pm\rangle = (|s_A\rangle|s_B\rangle \pm |t_A\rangle|t_B\rangle)/\sqrt{2}$ ;  $p_1 \sim (\Omega_N/\Delta_{dd})^2$  and  $p_0 \sim (\Omega_s/\Delta_{dd})^2$  are the small probabilities that erroneously generate a single excitation and vacuum contribution  $\rho_1$  and  $\rho_0$ , respectively, which are created due to double excitations (imperfect Rydberg blockade).

After linking the neighboring sites, we obtain a density matrix

$$\rho^0 = [1 - O(p_1)]\rho_2^0 + O(p_1)\rho_1, \quad (4)$$

up to the first order of  $O(p_1)$ , with a success probability of  $p \approx \frac{1}{2}\eta_r^2\eta_{\text{pd}}^2 e^{-L_0/L_{\text{att}}}[1 - O(p_1)]$ , where  $\rho_2^0 = F_0|\phi^+\rangle\langle\phi^+| + (1 - F_0)|\phi^-\rangle\langle\phi^-|$  up to a local unitary transformation, with  $F_0 = F_{\text{loc}}^2 + (1 - F_{\text{loc}})^2$ . The errors in the photonic channel are neglected since two-photon interference is used. The errors in the subsequent entanglement swapping step are similar to those of the local entanglement generation and can be estimated using the average error of the CNOT gate,

$$E_{\text{CNOT}} = 1 - F_{\text{CNOT}} = \frac{2\gamma\pi}{\Omega_s} + \frac{3\Omega_s^2}{2\Delta_{dd}^2}. \quad (5)$$

Figure 2(a) shows the optimized swapping errors  $E_{\text{CNOT}}$  versus  $\Delta_{dd}$  for  $\tau = 1/(2\pi\gamma) = 200$  and  $300 \mu\text{s}$ . The entanglement

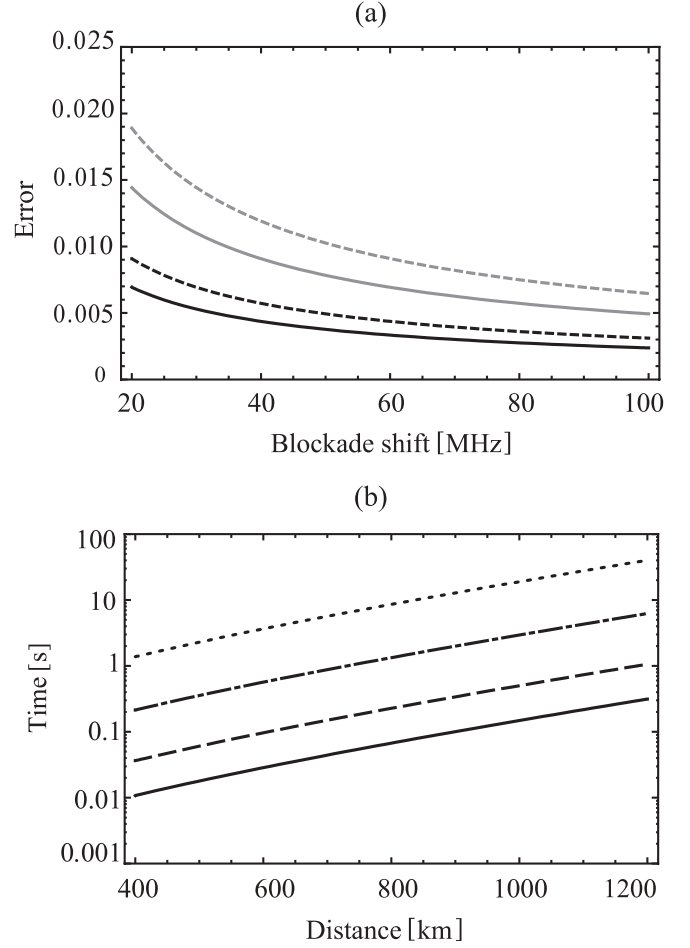


FIG. 2. (a) Average errors in local entanglement generation (gray) and entanglement swapping (black) versus dipole-dipole shift. The dashed and solid curves are for  $\tau = 200$  and  $300 \mu\text{s}$ , respectively. (b) Performance of the quantum repeater. The solid curve represents the result without entanglement purification, which requires local errors on the order of  $10^{-3}$ . The dashed and dot-dashed lines are the results for  $F_{\text{loc}} = F_{\text{CNOT}} = 0.99$  and  $0.98$ , where active entanglement purification is implemented twice and four times, respectively, when the fidelity is no larger than  $0.9$ . The final fidelity is higher than  $0.94$  and the probability of getting the entangled state is larger than  $0.95$  in both cases. The dotted line is the result of the best-known protocol with atomic ensembles and linear optics proposed in [5].

swapping errors are smaller than for the generation of local entanglement since no collective pulses with associated generation of collective excitations are required.

After  $n$ -step entanglement swapping, the mixed entangled state reads

$$\rho^n = [1 - O(p_1)]\rho_2^n + O(p_1)\rho_1, \quad (6)$$

where  $\rho_2^n = F_n|\phi^+\rangle\langle\phi^+| + (1 - F_n)|\phi^-\rangle\langle\phi^-|$ . The fidelity can be approximated by  $F_n = [F_{n-1}^2 + (1 - F_{n-1})^2]F_{\text{CNOT}}$ , for  $F_{\text{CNOT}}$  close to  $1$ . Note that the probability of obtaining the two excitations is independent of  $n$ , thanks to the use of qubit-type entanglement and the detection of two excitations in each step [4]. The success probability of each entanglement swapping step is  $p \approx [1 - O(2p_1)]\eta_d^2$ , where we have assumed for

simplicity that the probability to obtain a double Rydberg excitation during the entanglement swapping,  $(\Omega_s/\Delta_{dd})^2$ , is on the order of  $O(p_1)$ .

The local errors will accumulate during the entanglement connection [1]. A straightforward calculation shows that, for  $n = 4$  and  $F_{\text{loc}} = F_{\text{CNOT}} = 0.99$ , the final fidelity drops to  $F_4 = 0.69$ . Therefore, entanglement purification has to be performed, which can be achieved by employing two CNOT gates [21]. Assume we have generated two pairs of mixed entangled states between  $A_u$  and  $C_u$ , and  $A_d$  and  $C_d$ , described by  $\rho^i$ . We first apply a  $\pi/2$  Raman pulse coupling  $|s\rangle$  and  $|t\rangle$  to change the two excitation component to  $\rho_2^i = F_i|\phi^+\rangle\langle\phi^+| + (1 - F_i)|\psi^+\rangle\langle\psi^+|$  with  $|\psi^+\rangle = (|s_{A_u,d}\rangle|t_{C_u,d}\rangle + |t_{A_u,d}\rangle|s_{C_u,d}\rangle)/\sqrt{2}$ . We then perform two local CNOT gates with  $A_u$  and  $C_u$  as the control qubit and  $A_d$  and  $C_d$  as the target qubits, where we have assumed the two atomic ensembles at one site are located within the blockade radius. After the CNOT gates, we measure the target qubits in ensembles  $A_d$  and  $C_d$  in the  $|s\rangle$  and  $|t\rangle$  basis. If both qubits are in the  $|s\rangle$  or the  $|t\rangle$  state, the memory qubits in  $A_u$  and  $C_u$  are kept, otherwise the results are discarded. After entanglement purification, we obtain a mixed state  $\rho_2^p = F^p|\phi^+\rangle\langle\phi^+| + (1 - F^p)|\psi^+\rangle\langle\psi^+|$ , where the leakage to other states is neglected for large values of  $F_{\text{CNOT}}$ , and the achieved fidelity can be estimated as  $F^p = \frac{F_i^2}{F_i^2 + (1 - F_i)^2} F_{\text{CNOT}}^2$ . The success probability of purification is  $p \approx [F_i^2 + (1 - F_i)^2]\eta_d^2$ . After entanglement purification, the total density matrix can be described by

$$\rho = [1 - O(p_1/F_i^2)]\rho_2^p + O(p_1/F_i^2)\rho_1, \quad (7)$$

where we have assumed that the one excitation term only contributes a false signal.

The main result of our work is illustrated in Fig. 2(b), where the performance of the quantum repeater is plotted as a function of the communication distance for  $n = 4$ ,  $\eta_r = \eta_{\text{pd}} = 0.9$ ,  $\eta_d = 0.95$ ,  $L_{\text{att}} = 22$  km, and  $c = 2 \times 10^5$  km/s in fibers. For comparison, we also show the performance of the best-known atomic-ensemble-based repeater protocol without purification [5]. It can be seen that the entanglement distribution rate is enhanced by up to two orders of magnitude. For  $L = 1000$  km, the total time needed is on the order of a few hundred milliseconds.

#### IV. IMPLEMENTATION

The presented quantum repeater can be implemented using cold alkali metal atoms. Individual addressing of different sublevels can be achieved by choosing suitable laser polarization and applying a constant magnetic field. The atoms

may be trapped in a one-dimensional optical lattice generated by two counterpropagating laser beams, where in each well a mesoscopic atomic ensemble can be trapped and the size and distance of the wells can be controlled by tuning the angle between the trapping light fields [22].

In our protocol, we suggest the use of isotropic repulsive van der Waals interactions by exciting the atoms to Rydberg to  $s$  states with a principal quantum number  $n$  around 70. In this case, the interaction energy between two atoms at a distance of  $r$  can be approximated by  $V = -c_1 \frac{n^{12}}{r^6} + c'_1 \frac{n^{16}}{r^8}$  [23], with  $c_1 < 0$  and  $c'_1 > 0$ , where interactions proportional to  $1/r^{10}$  are neglected. The interactions are repulsive for large  $r$  and attractive for small  $r$ , yielding a critical distance  $r_c$  where the repulsive shift is maximal. We use  $r_c$  to estimate the minimum distance required to ensure repulsive interatomic interactions, and we find, for Rb,  $c_1 = -0.85$  and  $c'_1 = 0.8$ , and  $n = 70$ , a critical distance  $r_c = 0.3 \mu\text{m}$ , corresponding to a density of  $1/(r_c^3) = 3.7 \times 10^{13} \text{ cm}^{-3}$ . For a fixed density, one is interested in maximizing the number  $N$  of atoms within the blockade radius for high photon retrieval efficiencies and uncertainty in the atom number. As illustrated in Fig. 2(a), an interaction energy shift  $\Delta_{dd} > 20$  MHz allows for local errors of less than 2%. This yields a maximum Rydberg blockade radius  $R_b \approx (-\frac{c_1 n^{12}}{\Delta_{dd}})^{1/6}$ ; a more accurate calculation using the interaction energy in [23] gives  $R_b < 6 \mu\text{m}$  for  $n = 70$ . Thereby, a diameter of 2–3  $\mu\text{m}$  is sufficient for achieving high-fidelity local operations. [A density of  $3 \times 10^{13} \text{ cm}^{-3}$  and a volume of  $(2 \mu\text{m})^3$  would allow for about  $N = 240$  atoms per ensemble.] With the help of a bad cavity, the retrieval efficiency can be estimated as  $\eta_r = \frac{C}{C+1}$ , where  $C = N c_r^2 \frac{24F}{2\pi k^2 w_0^2}$  with  $k$  the wave number of the emitted photon and  $c_r$  the transition coefficient [24]. For a finesse of  $F = 100$ , cavity mode width  $w_0 = 5 \mu\text{m}$ ,  $c_r = \frac{1}{3}$ , and  $k = 2\pi/\mu\text{m}$ , we can obtain a high retrieval efficiency of 0.91.

Finally, to implement long-distance quantum communication over 1000 km, the coherence times of the quantum memory have to be on the order of a few hundred milliseconds. This should be achievable for an atomic memory with cold atoms, where a storage time of about 1 s for classical light has been achieved [25].

*Note added.* We are aware of an independent and similar work by Han *et al.* [26].

#### ACKNOWLEDGMENTS

We thank Z.-S. Yuan and R. Löw for helpful discussions. Financial support by the Austrian Science Foundation (FWF) through SFB FOQUS, and the European Union projects SCALA and NAMEQUAM, is acknowledged.

- [1] H.-J. Briegel, W. Dur, J. I. Cirac, and P. Zoller, *Phys. Rev. Lett.* **81**, 5932 (1998).  
 [2] L. Childress, J. M. Taylor, A. S. Sorensen, and M. D. Lukin, *Phys. Rev. Lett.* **96**, 070504 (2006); P. van Loock, T. D. Ladd, K. Sanaka, F. Yamaguchi, K. Nemoto, W. J. Munro, and Y. Yamamoto, *ibid.* **96**, 240501 (2006).  
 [3] L. M. Duan *et al.*, *Nature* **414**, 413 (2001).

- [4] B. Zhao, Z. B. Chen, Y. A. Chen, J. Schmiedmayer, and J. W. Pan, *Phys. Rev. Lett.* **98**, 240502 (2007); Z.-B. Chen, B. Zhao, Y. A. Chen, J. Schmiedmayer, and J. W. Pan, *Phys. Rev. A* **76**, 022329 (2007); L. Jiang, J. M. Taylor, and M. D. Lukin, *ibid.* **76**, 012301 (2007).  
 [5] N. Sangouard, C. Simon, B. Zhao, Y. A. Chen, H. deRiedmatten, J. W. Pan, and N. Gisin, *Phys. Rev. A* **77**, 062301 (2008).

- [6] M. Gao, L. M. Liang, C. Z. Li, and X. B. Wang, *Phys. Rev. A* **79**, 042301 (2009); Z.-Q. Yin, Y. B. Zhao, Y. Yang, Z. F. Han, and G. C. Guo, *ibid.* **79**, 044302 (2009).
- [7] D. N. Matsukevich and A. Kuzmich, *Science* **306**, 663 (2004); C.-W. Chou *et al.*, *Nature* **438**, 828 (2005); *Science* **316**, 1316 (2007); Y.-A. Chen *et al.*, *Nat. Phys.* **4**, 103 (2008); Z.-S. Yuan *et al.*, *Nature* **454**, 1098 (2008).
- [8] B. Zhao *et al.*, *Nat. Phys.* **5**, 95 (2009); R. Zhao *et al.*, *ibid.* **5**, 100 (2009).
- [9] N. Sangouard *et al.*, e-print [arXiv:0906.2699](https://arxiv.org/abs/0906.2699).
- [10] K. Hammerer, A. Sorensen, and E. Polzik, *Rev. Mod. Phys.* **82**, 1041 (2010).
- [11] D. Jaksch, J. I. Cirac, P. Zoller, S. L. Rolston, R. Cote, and M. D. Lukin, *Phys. Rev. Lett.* **85**, 2208 (2000); M. D. Lukin, M. Fleischhauer, R. Cote, L. M. Duan, D. Jaksch, J. I. Cirac, and P. Zoller, *ibid.* **87**, 037901 (2001).
- [12] E. Brion, K. Molmer, and M. Saffman, *Phys. Rev. Lett.* **99**, 260501 (2007).
- [13] M. Müller, I. Lesanovsky, H. Weimer, H. P. Buchler, and P. Zoller, *Phys. Rev. Lett.* **102**, 170502 (2009).
- [14] E. Urban *et al.*, *Nat. Phys.* **5**, 110 (2009); A. Gaëtan *et al.*, *ibid.* **5**, 115 (2009).
- [15] T. Wilk *et al.*, *Phys. Rev. Lett.* **104**, 010502 (2010); L. Isenhower, E. Urban, X. L. Zhang, A. T. Gill, T. Henage, T. A. Johnson, T. G. Walker, and M. Saffman, *ibid.* **104**, 010503 (2010).
- [16] T. Cubel Liebisch, A. Reinhard, P. R. Berman, and G. Raithel, *Phys. Rev. Lett.* **95**, 253002 (2005); A. K. Mohapatra, T. R. Jackson, and C. S. Adams, *ibid.* **98**, 113003 (2007); H. Weimer, R. Low, T. Pfau, and H. P. Buchler, *ibid.* **101**, 250601 (2008); H. Kübler *et al.*, e-print [arXiv:0908.0275v1](https://arxiv.org/abs/0908.0275v1).
- [17] N. Sangouard, R. Dubessy, and C. Simon, *Phys. Rev. A* **79**, 042340 (2009).
- [18] L. H. Pedersen and K. Mølmer, *Phys. Rev. A* **79**, 012320 (2009).
- [19] M. Saffman and T. G. Walker, *Phys. Rev. A* **72**, 022347 (2005).
- [20] C. Guerlin *et al.*, *Nature* **448**, 889 (2007).
- [21] C. H. Bennett, G. Brassard, S. Popescu, B. Schumacher, J. A. Smolin, and W. K. Wootters, *Phys. Rev. Lett.* **76**, 722 (1996); D. Deutsch, A. Ekert, R. Jozsa, C. Macchiavello, S. Popescu, and A. Sanpera, *ibid.* **77**, 2818 (1996).
- [22] L. Fallani *et al.*, *Opt. Exp.* **13**, 4303 (2005).
- [23] K. Singer *et al.*, *J. Phys. B* **38**, S295 (2005).
- [24] J. Simon, H. Tanji, J. K. Thompson, and V. Vuletic, *Phys. Rev. Lett.* **98**, 183601 (2007).
- [25] R. Zhang, S. R. Garner, and L. V. Hau, *Phys. Rev. Lett.* **103**, 233602 (2009); U. Schnorrberger, J. D. Thompson, S. Trotzky, R. Pugatch, N. Davidson, S. Kuhr, and I. Bloch, *ibid.* **103**, 033003 (2009).
- [26] Y. Han, B. He, K. Heshami, C.-Z. Li, and C. Simon, *Phys. Rev. A* **81**, 052311 (2010).